Measurements in Fluid Mechanics

Introduction

The purpose of this chapter is to provide the reader with a basic introduction to the concepts and techniques applied by engineers who measure flow parameters either in the laboratory or in an industrial environment.

Methods and instrumentation employed to measure pressure, velocity, and discharge are presented.

Measurement of Local Flow Parameters

Dynamic Response and Averaging

Pressure

- Manometer
- Bourdon Gage

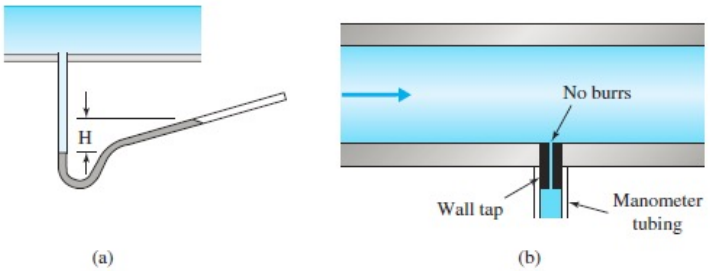

Manometer used to measure pressure: (a) inclined tube manometer; (b) piezometer opening.

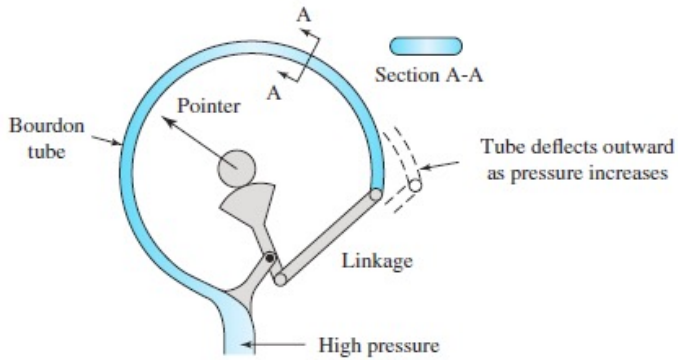

Bourdon tube pressure gage.

Measurement of Local Flow Parameters

Pressure Transducer

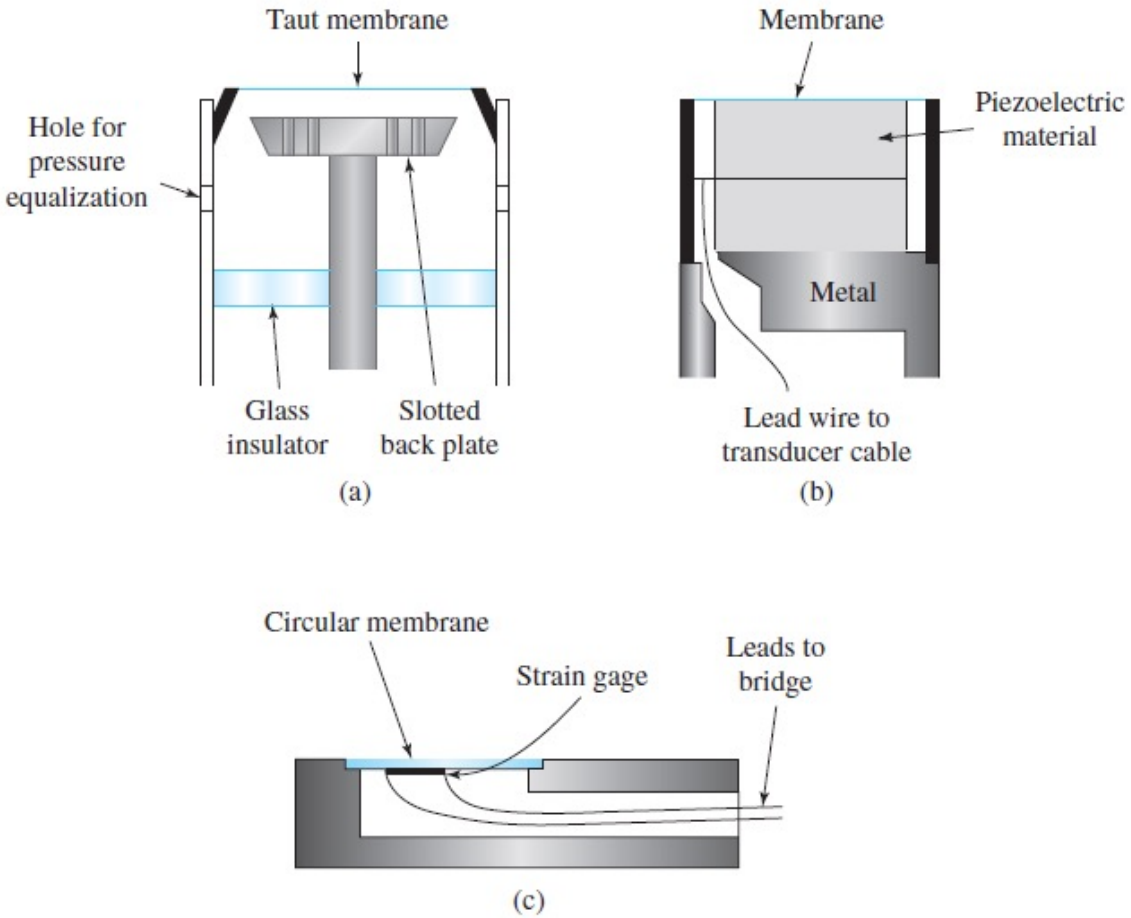

Pressure transducers: (a) condenser microphone; (b) piezoelectric pressure transducer; (c) strain-gage transducer.

Measurement of Local Flow Parameters

Velocity

- Particle Velocity Measurement
- Pitot-Static Probe

$$V = \sqrt{\frac{2}{\rho}(p_T - p)}$$

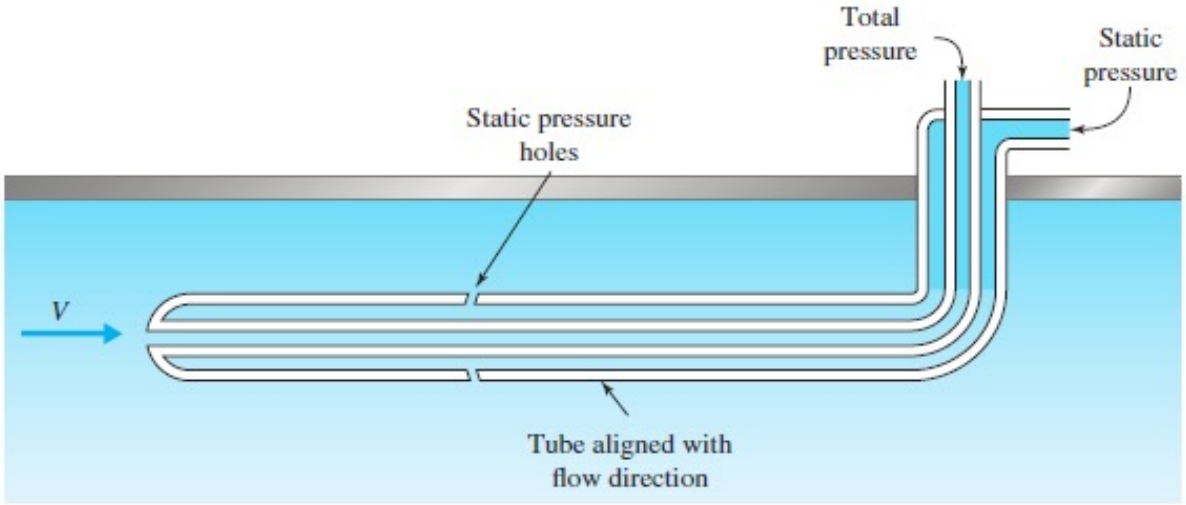

Pitot-static probe.

Measurement of Local Flow Parameters

Velocity

- Cup or Propeller Anemometer

Cup or propeller anemometers are employed to measure the velocity of either gases or liquids.

- Thermal Anemometer

The thermal (hot wire) anemometer is employed to measure velocity in air.

Measurement of Local Flow Parameters

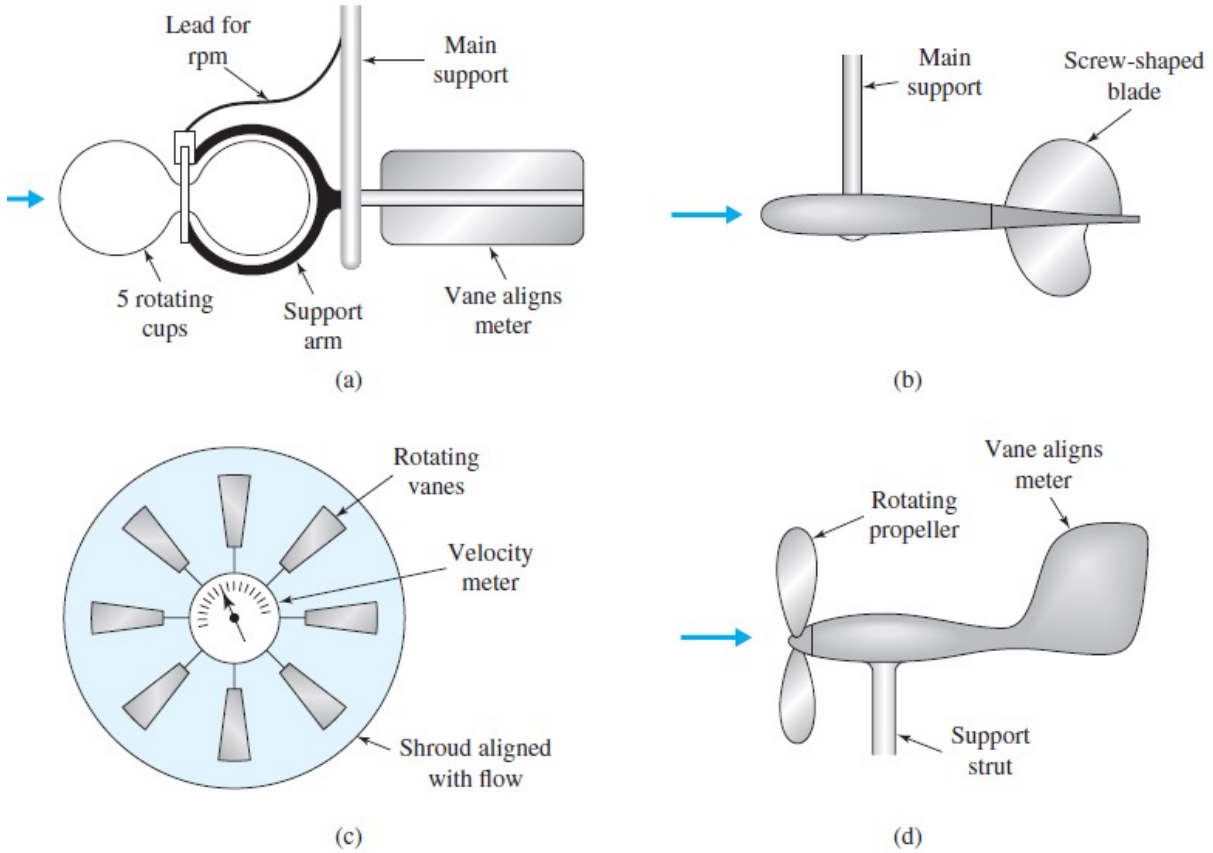

Anemometers: (a) current meter; (b) propeller anemometer; (c) ducted vane anemometer; (d) wind vane anemometer.

Measurement of Local Flow Parameters

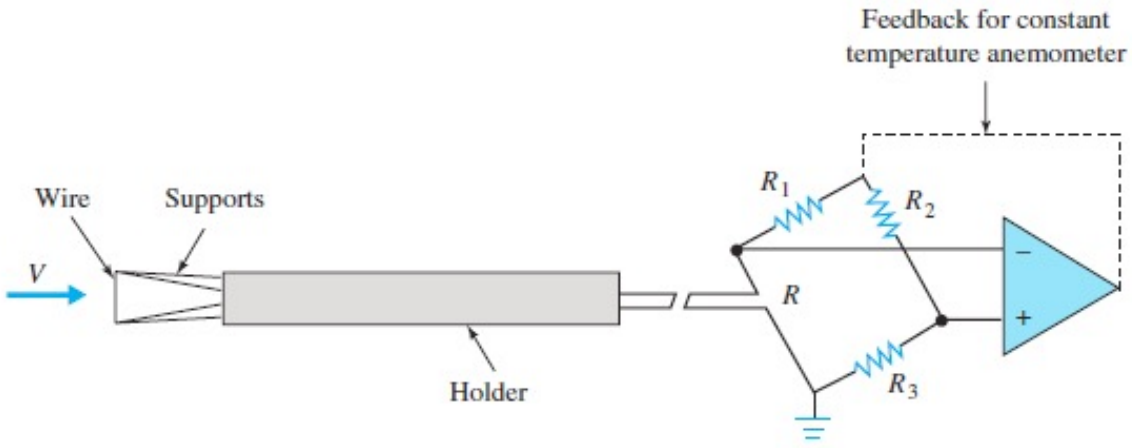

Thermal anemometer.

Measurement of Local Flow Parameters

- Laser-Doppler Velocimeter

A device that can be used advantageously when it is desired not to have the probe immersed in the flow is the laser-doppler velocimeter (LDV).

$$u = \frac{\Delta x}{\Delta t} = \frac{\lambda f}{2\sin(\theta/2)}$$

Measurement of Local Flow Parameters

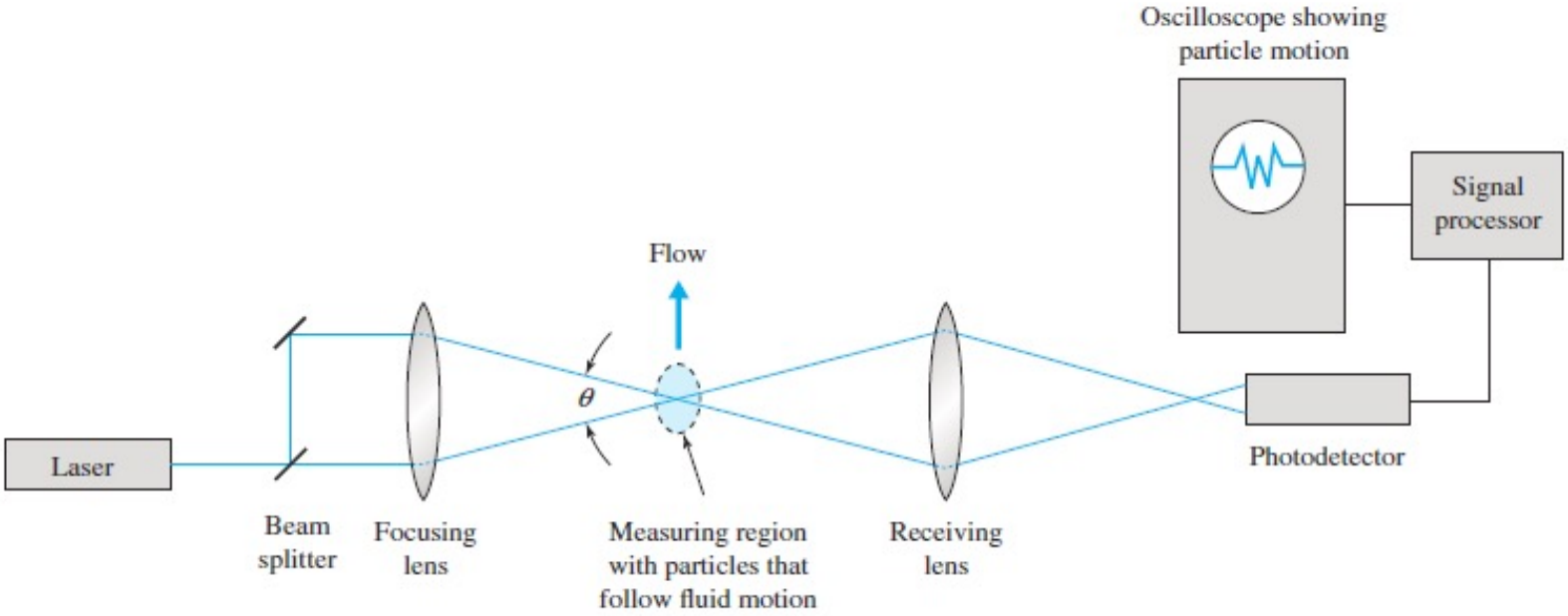

Dual-beam laser-doppler velocimeter.

Flow Rate Measurement

Velocity–Area Method

In a manner that does not require calibration and for steady flow, a velocity distribution can be measured by systematically moving a velocity probe throughout the flow cross section, or by using a so-called “rake” where local velocities are measured simultaneously.

Flow Rate Measurement

Differential Pressure Meters

Downstream of the restriction, the streamlines converge to form a minimal flow area A_c, termed the *vena contracta*.

$$\frac{V_1^2}{2g} + \frac{p_1}{\gamma} + z_1 = \frac{V_c^2}{2g} + \frac{p_c}{\gamma} + z_c$$

$$V_1 A_1 = V_c A_c$$

Flow Rate Measurement

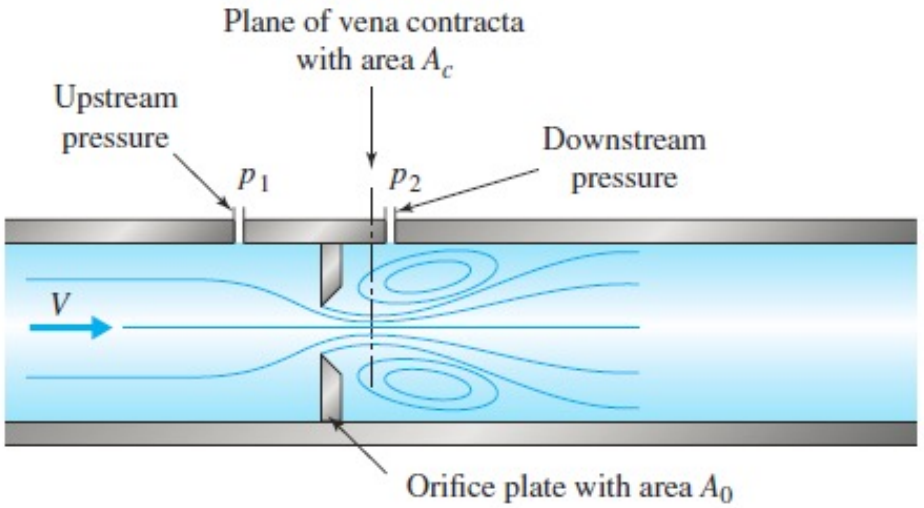

Flow through an orifice meter.

Flow Rate Measurement

$$Q = \frac{C_d A_0}{\sqrt{1 - (C_c A_0 / A_1)^2}} \sqrt{2g(h_1 - h_2)}$$

$$Q = K A_0 \sqrt{2g(h_1 - h_2)}$$

$$K = \frac{C_d}{\sqrt{1 - C_c^2 \beta^4}}$$

Flow Rate Measurement

Orifice Meter

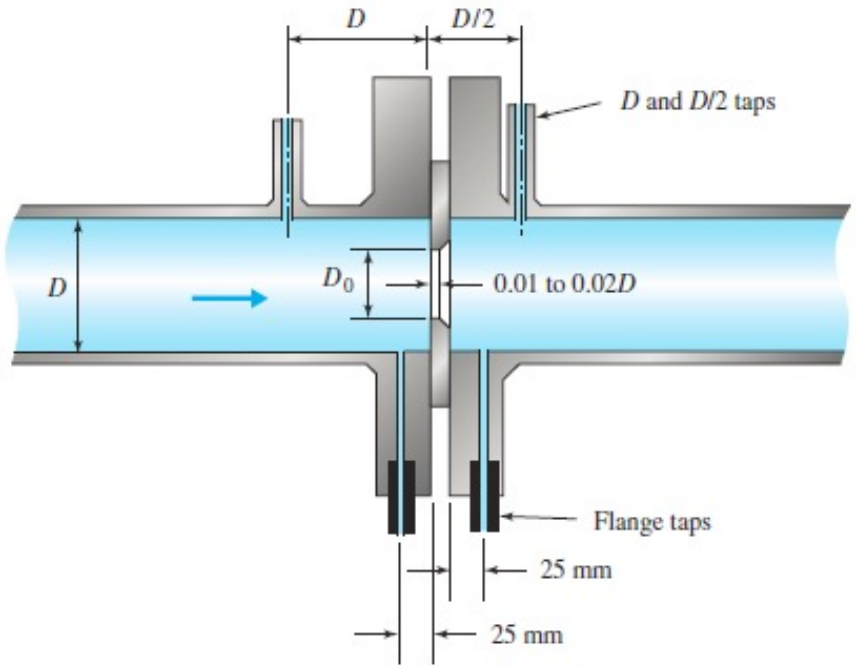

Details of a thin-plate orifice meter. (Based on G. E. Mattingly, *Fluid Mechanics Measurements*, 1996, Taylor & Francis Group LLC.)

Flow Rate Measurement

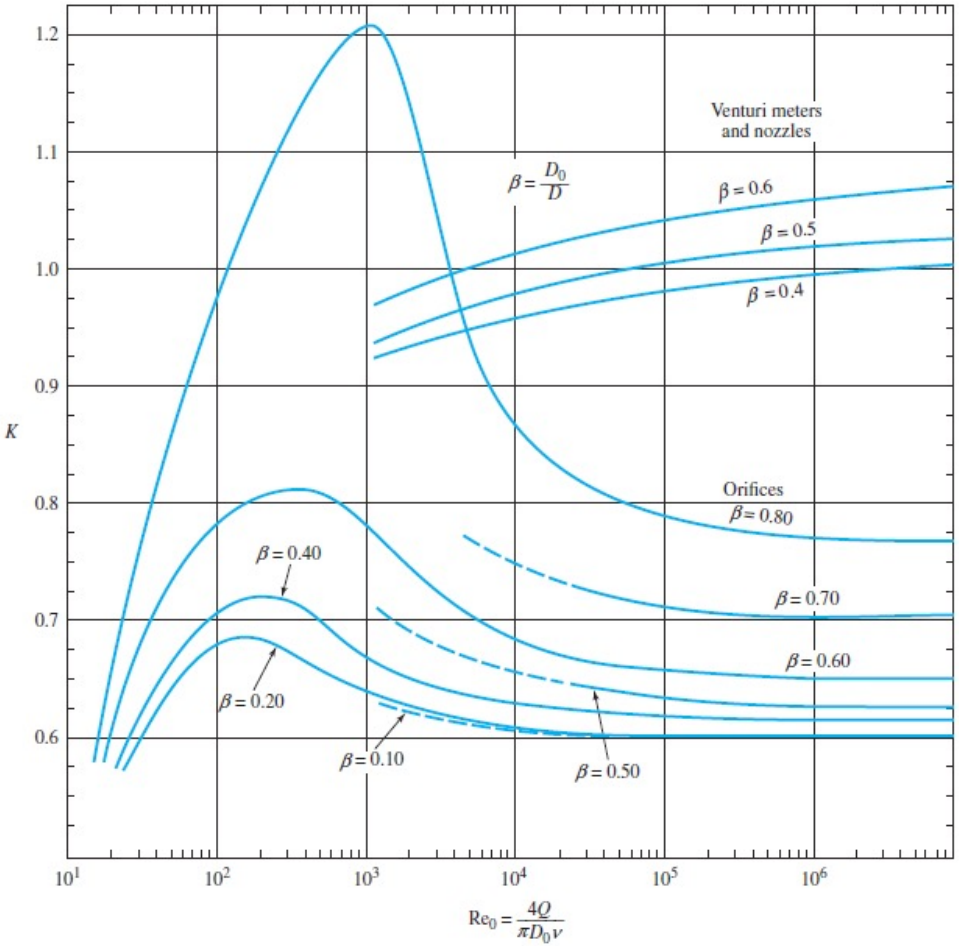

Flow coefficient K versus the Reynolds number for orifices, nozzles, and venturi meters. (Based on Robertson and Crowe, *Engineering Fluid Mechanics*, 1990, John Wiley & Sons, Inc.)

Flow Rate Measurement

Venturi Meter

The venturi meter has a shape that attempts to mimic the flow patterns through a streamlined obstruction in a pipe.

Flow Nozzle

The flow nozzle consists of a standardized shape with pressure taps typically located one diameter upstream of the inlet and one-half diameter downstream.

Flow Rate Measurement

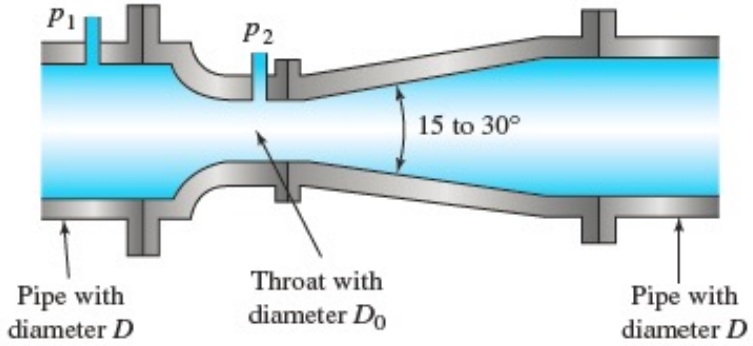

Venturi meter.

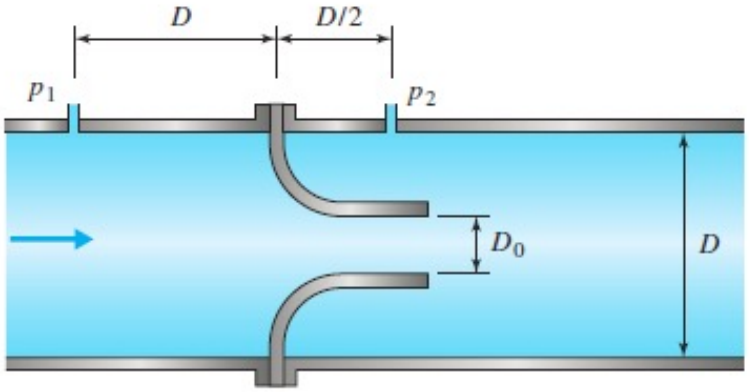

Flow nozzle.

Flow Rate Measurement

Elbow Meter

$$Q = KA\sqrt{\frac{R}{D}\frac{\Delta p}{\rho}}$$

$$K = 1 - \frac{6.5}{\sqrt{\mathrm{Re}}}$$

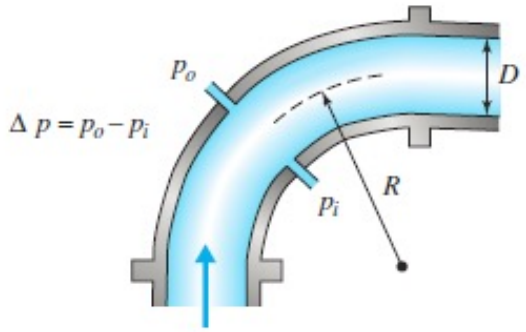

Elbow meter.

Flow Rate Measurement

Other Types of Flow Meters

Turbine Meter

The turbine meter consists of a propeller mounted inside a duct that is spun by the flowing fluid.

Rotameter

The rotameter consists of a tapered tube in which the flow is directed vertically upward.

Flow Rate Measurement

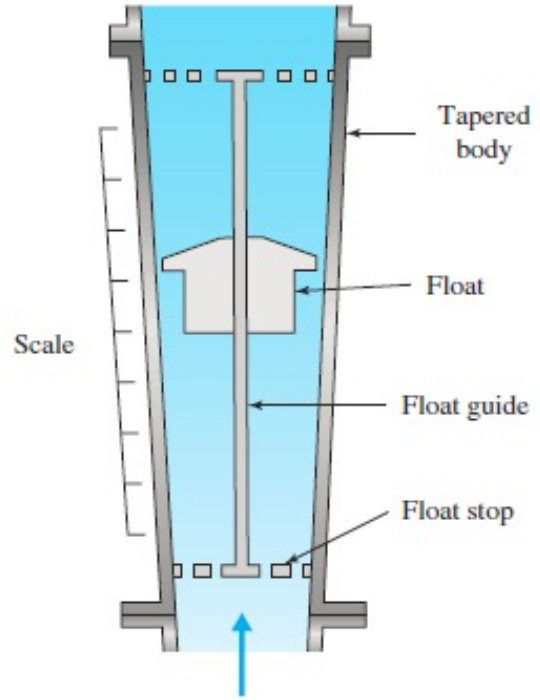

Rotameter.

Flow Rate Measurement

Target Meter

The target meter consists of a disk suspended on a support strut immersed in the flow.

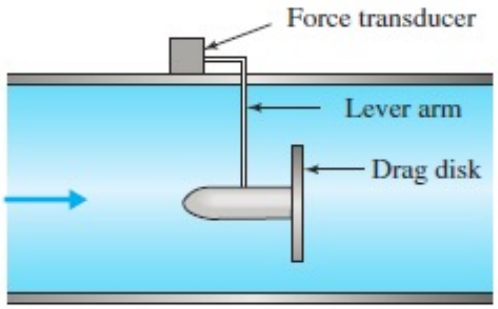

Target meter.

Flow Rate Measurement

Electromagnetic Flowmeter

The electromagnetic flowmeter is a nonintrusive device that consists of an arrangement of magnetic coils and electrodes encircling the pipe.

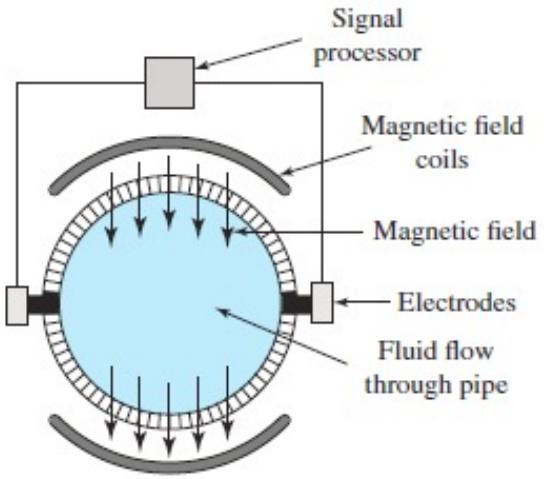

Electromagnetic flowmeter.

Flow Rate Measurement

Acoustic Flowmeter

Based on one of two principles:

- ultrasonic transmitters/receivers beamed across a flow path
- the Doppler effect.

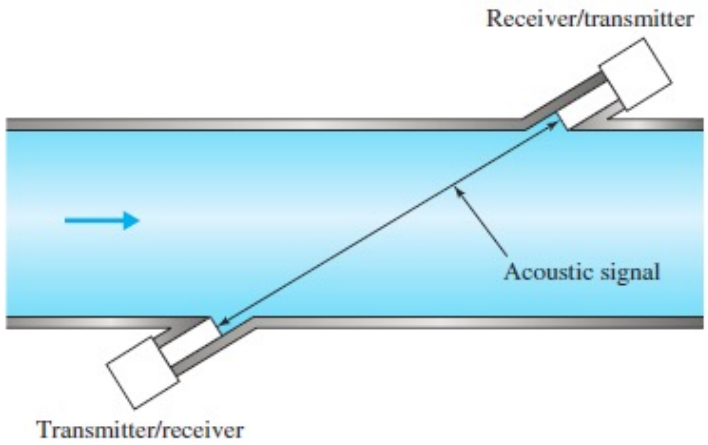

Acoustic flowmeter.

Flow Rate Measurement

Vortex-Shedding Meter

This flow-metering device consists of a single strut or series of struts placed chord-like inside a pipe normal to the flow direction.

Coriolis-Acceleration Flowmeter

These are meters that are based on the Coriolis acceleration principle.

Open-Channel Flowmeters

Flow Visualization

Examples include particles used to visualize pathlines in liquid flows around submerged objects, dye released to study the mixing process in a stream, smoke released at the upwind end of a wind tunnel to study the development of a boundary layer, and airflow patterns above a solid surface visualized by coating that surface with a viscous liquid.

A pathline is physically generated by following the motion of an individual particle such as a bubble or small neutrally buoyant sphere over a period of time.

Flow Visualization

Tracers

An effective tracer does not alter the flow pattern but is transported with the flow and is readily observable.

Hydrogen Bubbles: A very thin metallic wire can be placed in water to serve as the cathode of a direct-current circuit, with any suitable conductive material acting as an anode.

Usually, the hydrogen bubbles are used as the tracer since they are smaller than the oxygen bubbles and more of them are formed.

Flow Visualization

Hydrogen bubble streaklines showing separated flow around a rotating airfoil. (Koochesfahani, M. M. and Smiljanovski, V. [1993] "Effect of initial acceleration on the evolution of flow around an airfoil pitching to high angles of attack," *AIAA J.*, 31(8), 1529–1531. Courtesy of V. Smiljanovski and M. Koochesfahani.)

Flow Visualization

Chemical Indicators

A change in pH caused by the injection of a base solution changes the color of the liquid. The lifetime of the colored water depends on the molecular diffusion of the hydrogen ions and the turbulence.

Particles in Air

The method can be applied to flows where the Reynolds number based on the wire diameter is less than 20.

Flow Visualization

Velocimetry:

Velocimetry methods are particularly useful in the studies of explosions, transients in channels and ducts, flow in internal combustion engines, bubble growth and collapse, fluid-solid interaction, and the structure of turbulent flow.

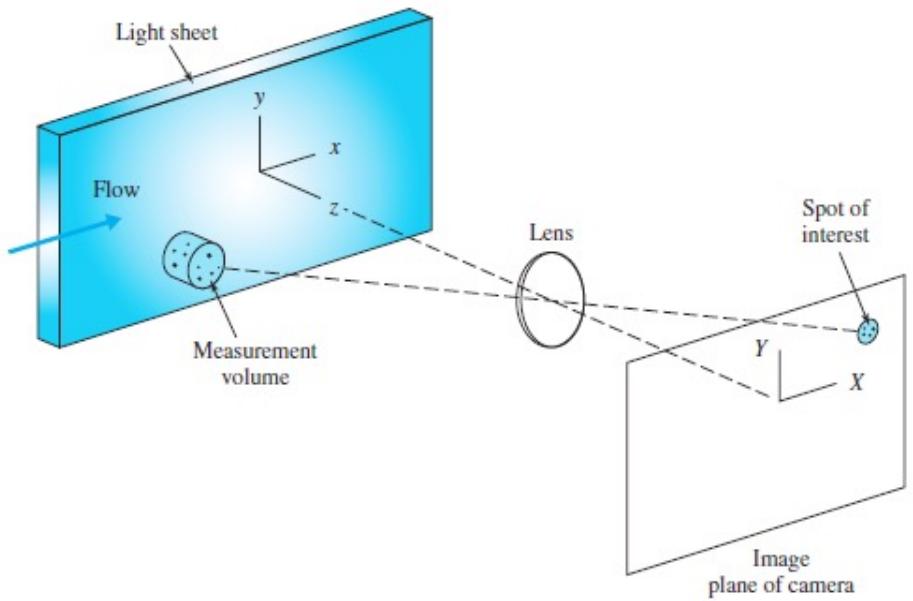

Pulsed light velocimeter. (Courtesy of R. Adrian.)

Flow Visualization

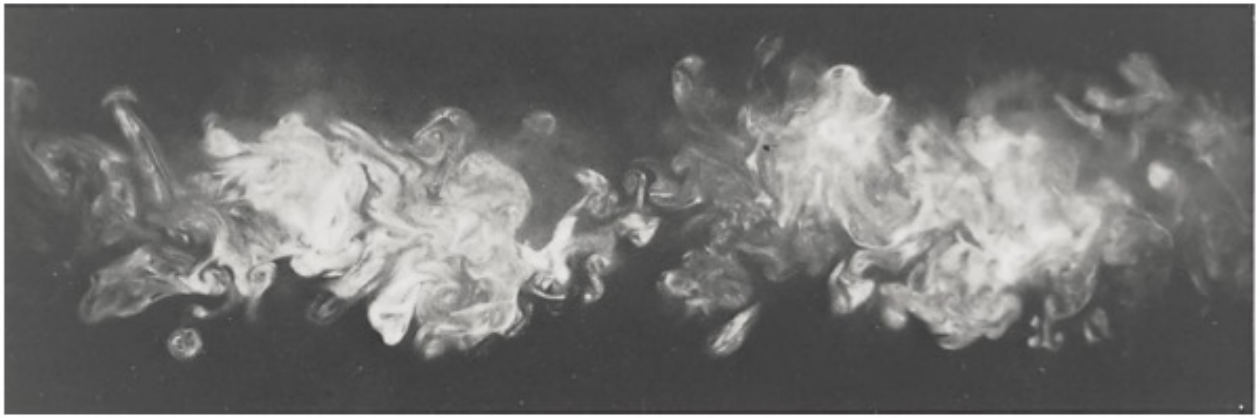

Turbulent wake behind a circular cylinder at Re = 1760.
(Courtesy of R. E. Falco.)

Tufts and Oil Films

Flow visualization along a surface can be accomplished by attaching tufts to the surface, or if flow away from the surface is to be observed, they may be supported on wires.

Flow Visualization

Photography and Lighting

(a)

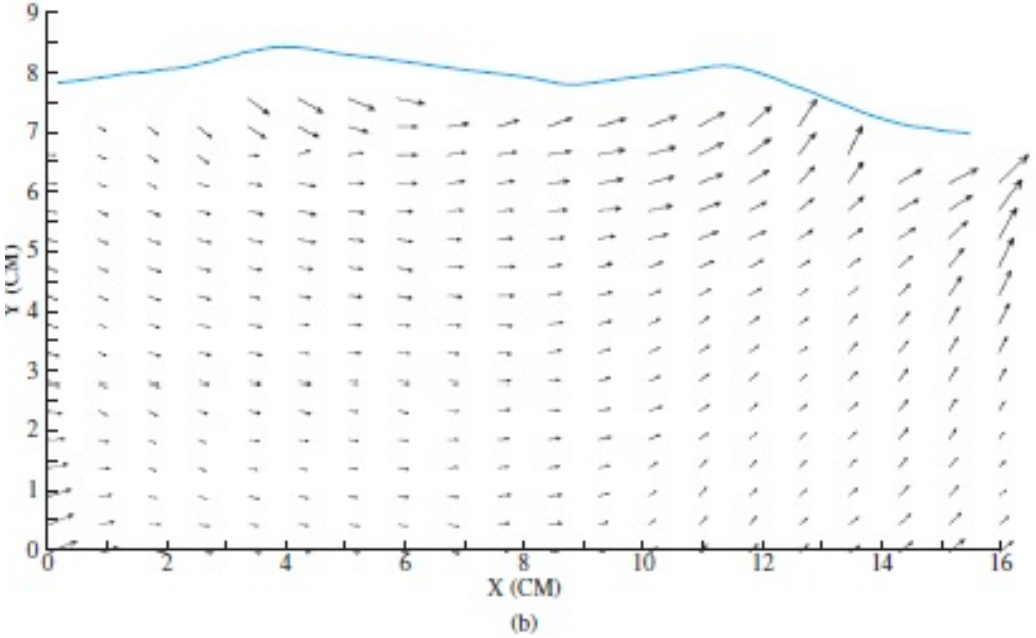

(b)

Particle Image Velocimetry (PIV): (a) photograph of particle pathlines; (b) scaled velocity vectors. (Courtesy of R. Bouwmeester.)

Flow Visualization

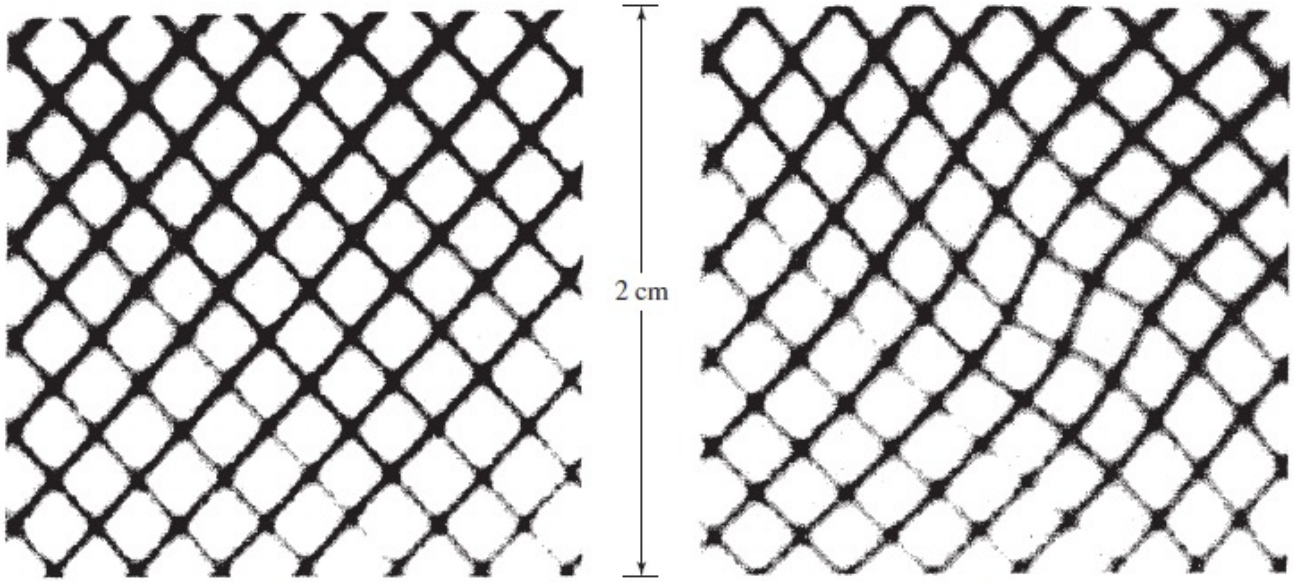

Molecular Tagging Velocimetry (MTV); (a) sample grid within a vortex ring just after laser tagging; (b) displaced grid 6 ms later; (c) velocity field of the vortex ring approaching a wall. (Gendrich, C. P., Koochesfahani, M. M. and Nocera, D. G. (1997.) "Molecular tagging velocimetry and other novel applications of a new phosphorescent supramolecule," *Exp. Fluids*, 23(5), 361–372. Courtesy of C. Gendrich and M. Koochesfahani.)

Flow Visualization

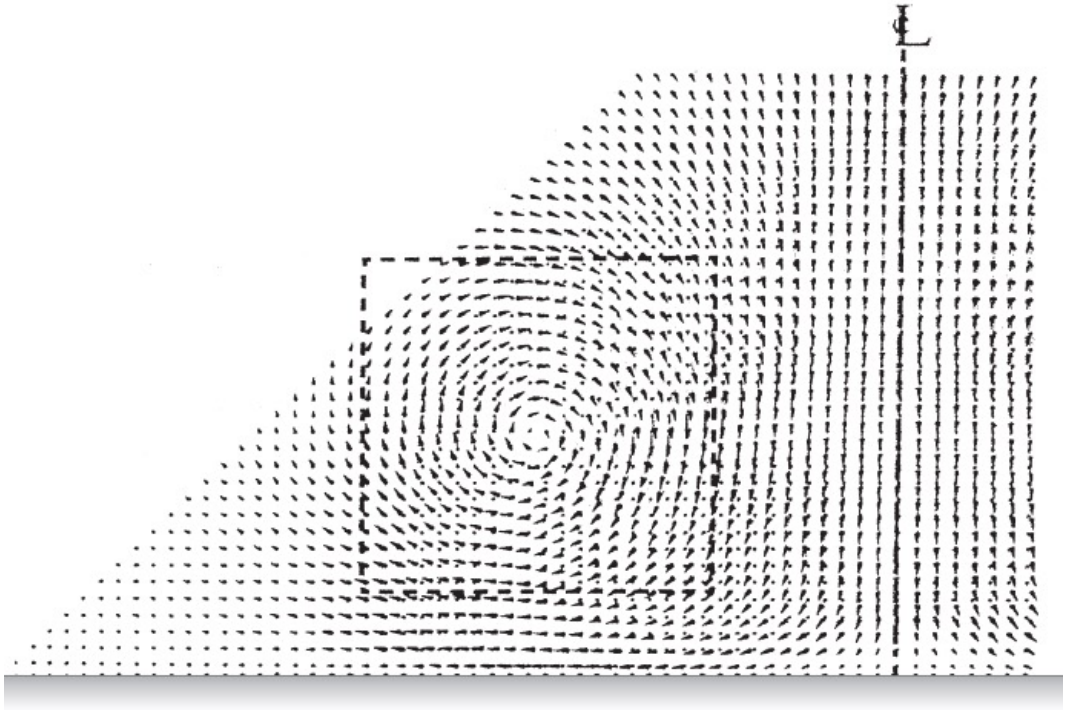

(c)

Molecular Tagging Velocimetry (MTV); (a) sample grid within a vortex ring just after laser tagging; (b) displaced grid 6 ms later; (c) velocity field of the vortex ring approaching a wall. (Gendrich, C. P., Koochesfahani, M. M. and Nocera, D. G. (1997.) "Molecular tagging velocimetry and other novel applications of a new phosphorescent supramolecule," *Exp. Fluids*, 23(5), 361–372. Courtesy of C. Gendrich and M. Koochesfahani.)

Flow Visualization

Laser Induced Fluorescence (LIF): (a) experimental layout; (b) detail of spanwise flow structure measured by LIF. (MacKinnon, C. G. and Koochesfahani, M. M. (1997.) "Flow structure and mixing in a low Reynolds number forced wake inside a confined channel," *Phys. Fluids*, 9(10), 3099-3101. Courtesy of C. MacKinnon and M. Koochesfahani.)

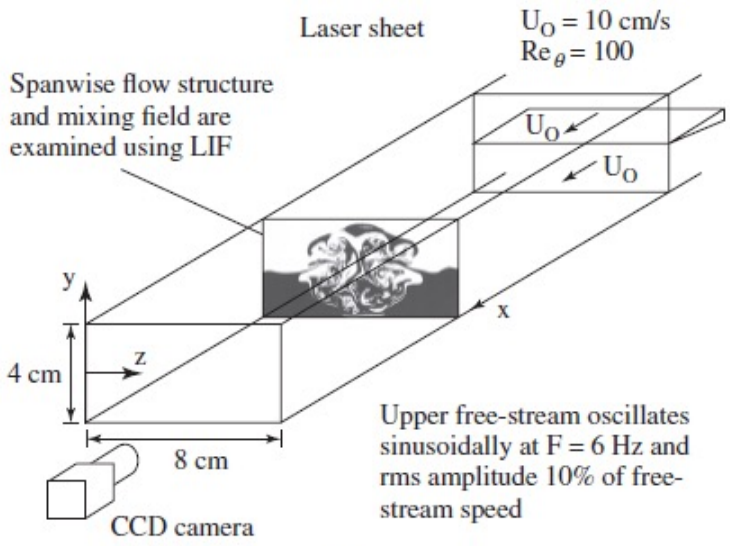

(a)

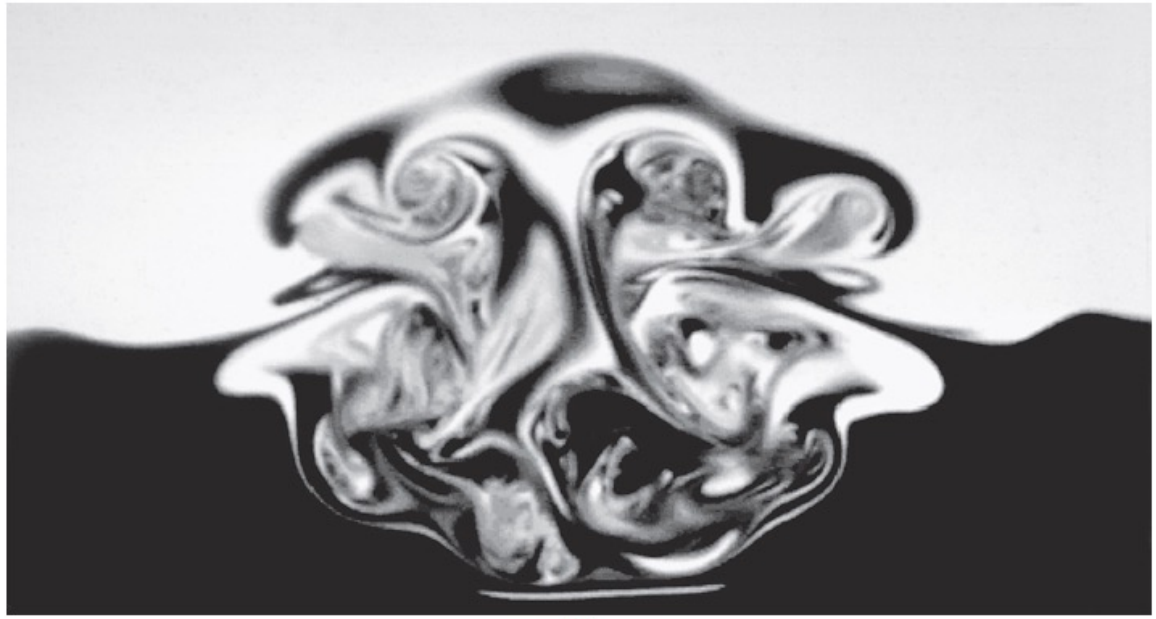

(b)

Flow Visualization

Index of Refraction Methods

The three index of refraction techniques are schlieren, shadowgraph, and interferometry.

The methods depend on the variation of the index of refraction in a transparent fluid medium and the resulting deflection of a light beam directed through the medium.

The index of refraction is a function of the thermodynamic state of the fluid and typically depends only on the density.

Flow Visualization

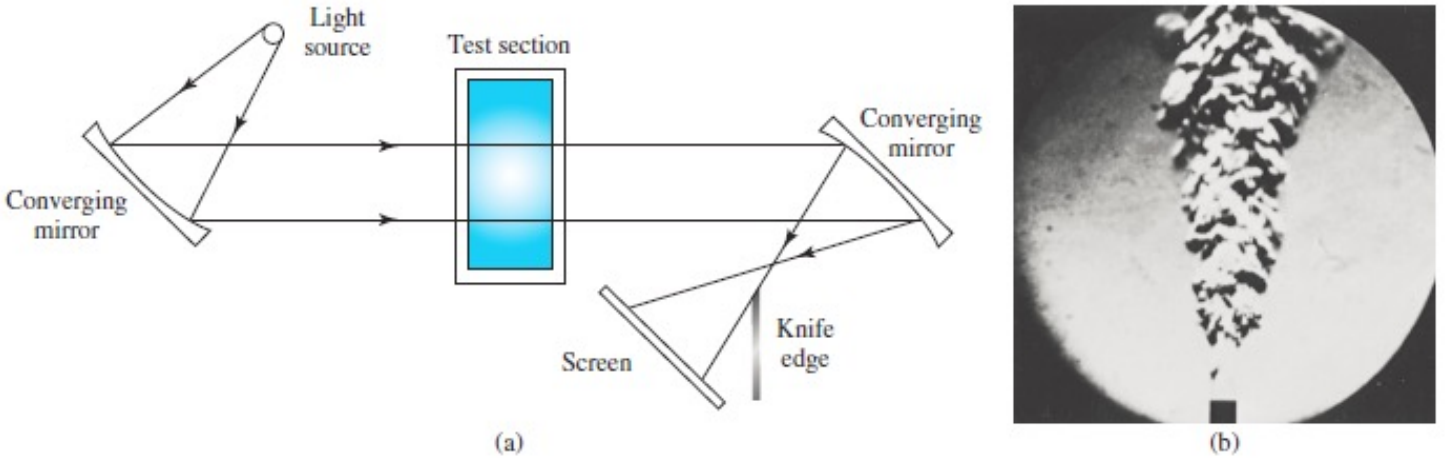

Schlieren system: (a) schematic; (b) helium jet entering atmospheric air. (Courtesy of R. Goldstein.)

Flow Visualization

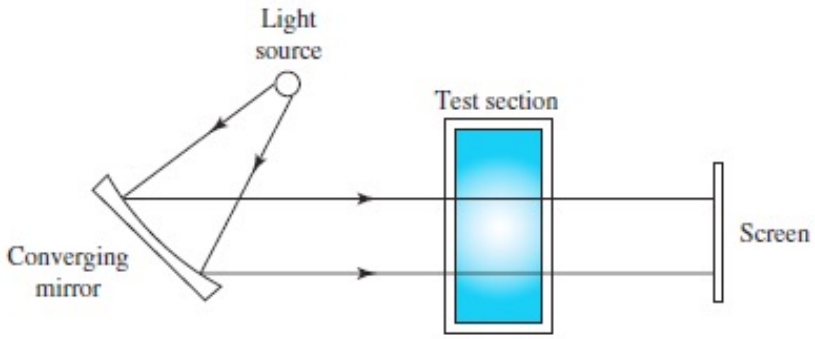

(a)

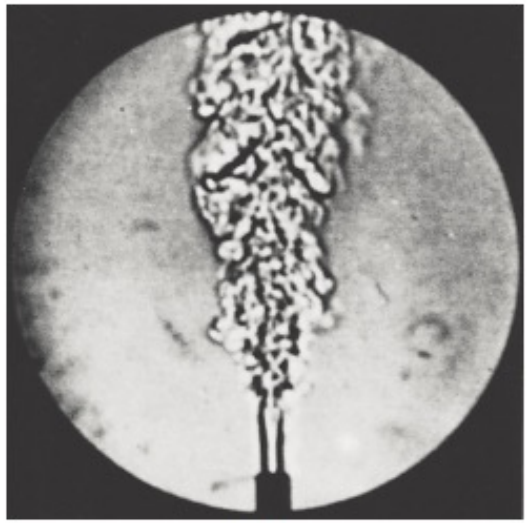

(b)

Shadowgraph system: (a) schematic; (b) helium jet entering atmospheric air.
(Courtesy of R. Goldstein.)

Flow Visualization

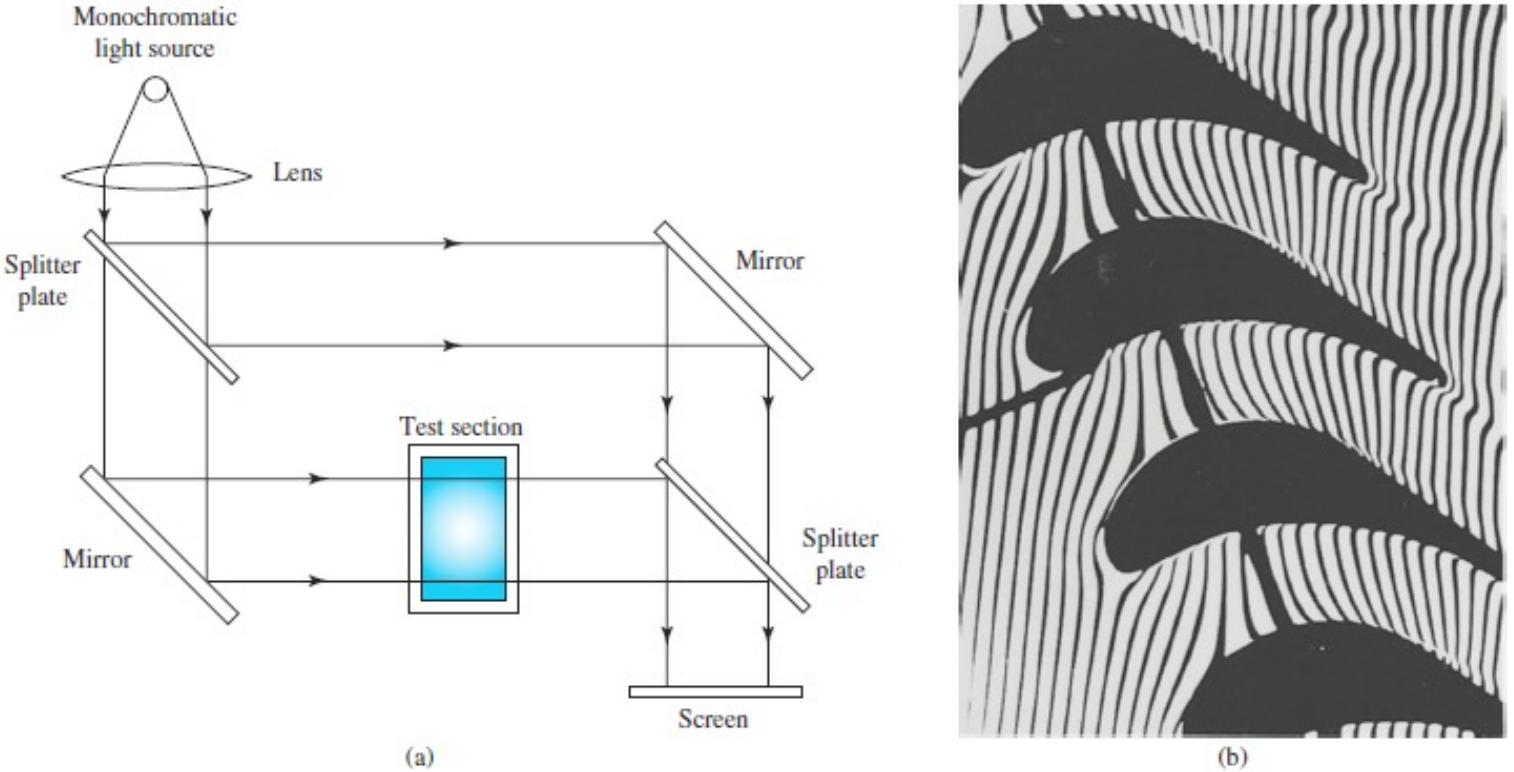

Mach–Zehnder interferometer: (a) schematic; (b) flow over heated gas-turbine blades. (Courtesy of R. Goldstein.)

Data Acquisition and Analysis

Digital Recording of Data

Examples include reading a manometer attached to an orifice flowmeter, monitoring a digital rpm readout of a vane anemometer, and recording the pressure indicated on a Bourdon gage.

The advent of the personal computer has revolutionized automated acquisition of flow data.

Data Acquisition and Analysis

Uncertainty Analysis

An *error* is the fixed, unchangeable difference between the true value and the recorded value, whereas an *uncertainty* is the statistical value that an error may assume for any given measurement.

Uncertainty can be divided into three categories: (1) uncertainty due to calibration of instruments, (2) uncertainty due to acquisition of data, and (3) uncertainty as a result of data reduction.

Data Acquisition and Analysis

Precision is alternatively termed repeatability; it is found by taking repeated measurements from the parameter population and using the standard deviation as a precision index.

The parameter x_i is one particular measured variable, or measurand, $<x_i>$ is the average of all the measured variables, and δx_i is the uncertainty interval, or precision, associated with x_i.

$$x_i = <x_i> \pm \delta x_i$$

Data Acquisition and Analysis

In addition to defining uncertainties in the data, it is necessary to propagate those uncertainties into the results.

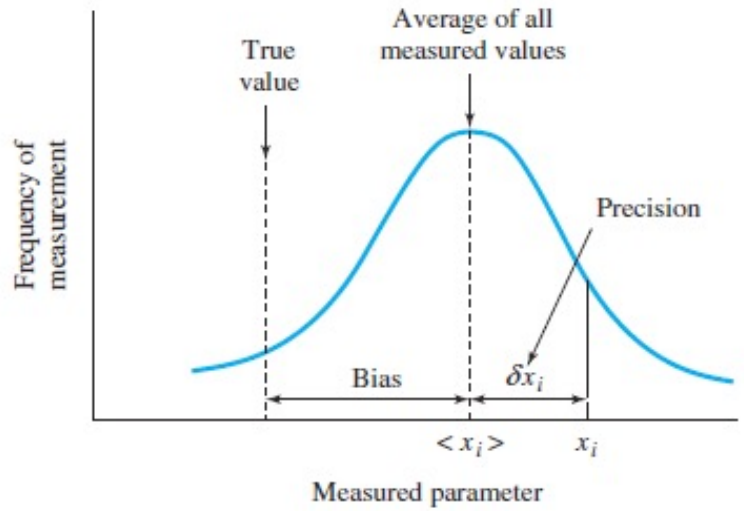

Uncertainties associated with a sampling of data.

Data Acquisition and Analysis

Discharge and pressure data are collected for water flow through an orifice meter in the pipe of Figure E13.1a. The orifice diameter is 35.4 mm, and the diameter of the pipe is 50.8 mm. The original data are reduced to the form shown in the accompanying table. The second column is the discharge Q; the precision δQ (zero bias, $P = 0.95$) is given in the third column; and the pressure head data $\Delta h = h_1 - h_2$ are presented in the fourth column. In addition, the precision for each of the pressure measurements is determined to be the same, namely, $\delta(\Delta h) = 0.025$ m (zero bias, $P = 0.95$). The fifth and sixth columns show the Reynolds numbers and the flow coefficient K computed using Eq. 13.3.8. Determine the uncertainties in the result K as a result of the estimated uncertainties in the measurands Q and Δh.

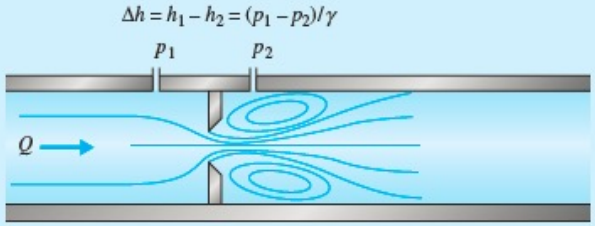

Figure E13.1a

Solution

Equation 13.3.8 is used in conjunction with Eq. 13.5.4 to propagate the uncertainties from Q and Δh into K. For example, consider the data for $i = 6$. Calculation of δK proceeds as follows. The orifice area is

$$A_0 = \frac{\pi}{4} 0.0354^2 = 9.84 \times 10^{-4} \text{ m}^2$$

Data no. i	Q (m^3/s)	δQ (m^3/s)	Δh (m)	Re	K	δK
1	0.00119	0.00010	0.139	42 800	0.732	0.085
2	0.00162	0.00012	0.265	58 300	0.722	0.062
3	0.00200	0.00015	0.403	71 900	0.723	0.058
4	0.00223	0.00015	0.517	80 200	0.711	0.051
5	0.00251	0.00015	0.655	90 300	0.711	0.045
6	0.00276	0.00017	0.781	99 300	0.716	0.046
7	0.00294	0.00018	0.907	105 700	0.708	0.045
8	0.00314	0.00019	1.008	112 900	0.717	0.045
9	0.00330	0.00016	1.134	118 700	0.711	0.035
10	0.00346	0.00017	1.247	124 400	0.711	0.036
11	0.00373	0.00017	1.386	134 200	0.727	0.034
12	0.00382	0.00017	1.512	137 400	0.713	0.032
13	0.00408	0.00018	1.663	146 700	0.726	0.033
14	0.00424	0.00019	1.852	152 500	0.715	0.032
15	0.00480	0.00021	2.293	172 600	0.727	0.032

Data Acquisition and Analysis

and the diameter ratio is

$$\beta = \frac{35.4}{50.8} = 0.697 \simeq 0.7$$

With Eq. 13.3.8, values of K are determined for $(Q, \Delta h)$, $(Q + \delta Q, \Delta h)$, and $(Q, \Delta h + \delta(\Delta h))$:

$$K(Q, \Delta h) = \frac{0.00276}{9.84 \times 10^{-4}\sqrt{2 \times 9.81 \times 0.781}} = 0.716$$

$$K(Q + \delta Q, \Delta h) = \frac{0.00276 + 0.00017}{9.84 \times 10^{-4}\sqrt{2 \times 9.81 \times 0.781}} = 0.761$$

$$K(Q, \Delta h + \delta(\Delta h)) = \frac{0.00276}{9.84 \times 10^{-4}\sqrt{2 \times 9.81 \times (0.781 + 0.025)}} = 0.705$$

These are then substituted into Eq. 13.5.4, with the variable K replacing the result R in that relation:

$$\begin{aligned}\delta K &= \{[K(Q + \delta Q, \Delta h) - K(Q, \Delta h)]^2 + [K(Q, \Delta h + \delta(\Delta h)) - K(Q, \Delta h)]^2\}^{1/2} \\ &= [(0.761 - 0.716)^2 + (0.705 - 0.716)^2]^{1/2} \\ &= 0.046\end{aligned}$$

The results for all measurands are similarly evaluated and shown in the last column in the table. In addition, they are plotted in Figure E13.1b, where the vertical lines, or uncertainty bands, associated with each value of K have the magnitude of $2\delta K$. The bands can be interpreted as the estimated precision for K, based on zero bias and $P = 0.95$ for the two measurands. Note that the precision δK stabilizes at approximately 0.032 at the higher Reynolds numbers and that the magnitude of δK is greater at lower Reynolds numbers. An alternative way to express this is that the uncertainty of K decreases with increasing Reynolds number. The data in the figure should be compared with the orifice curve labeled $\beta = 0.7$ in Figure 13.10.

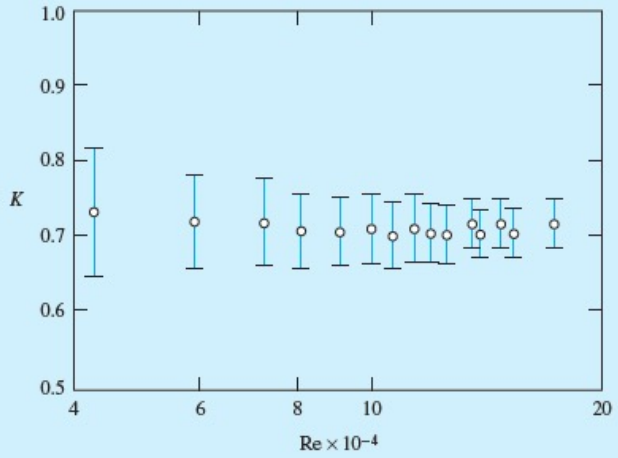

Data Acquisition and Analysis

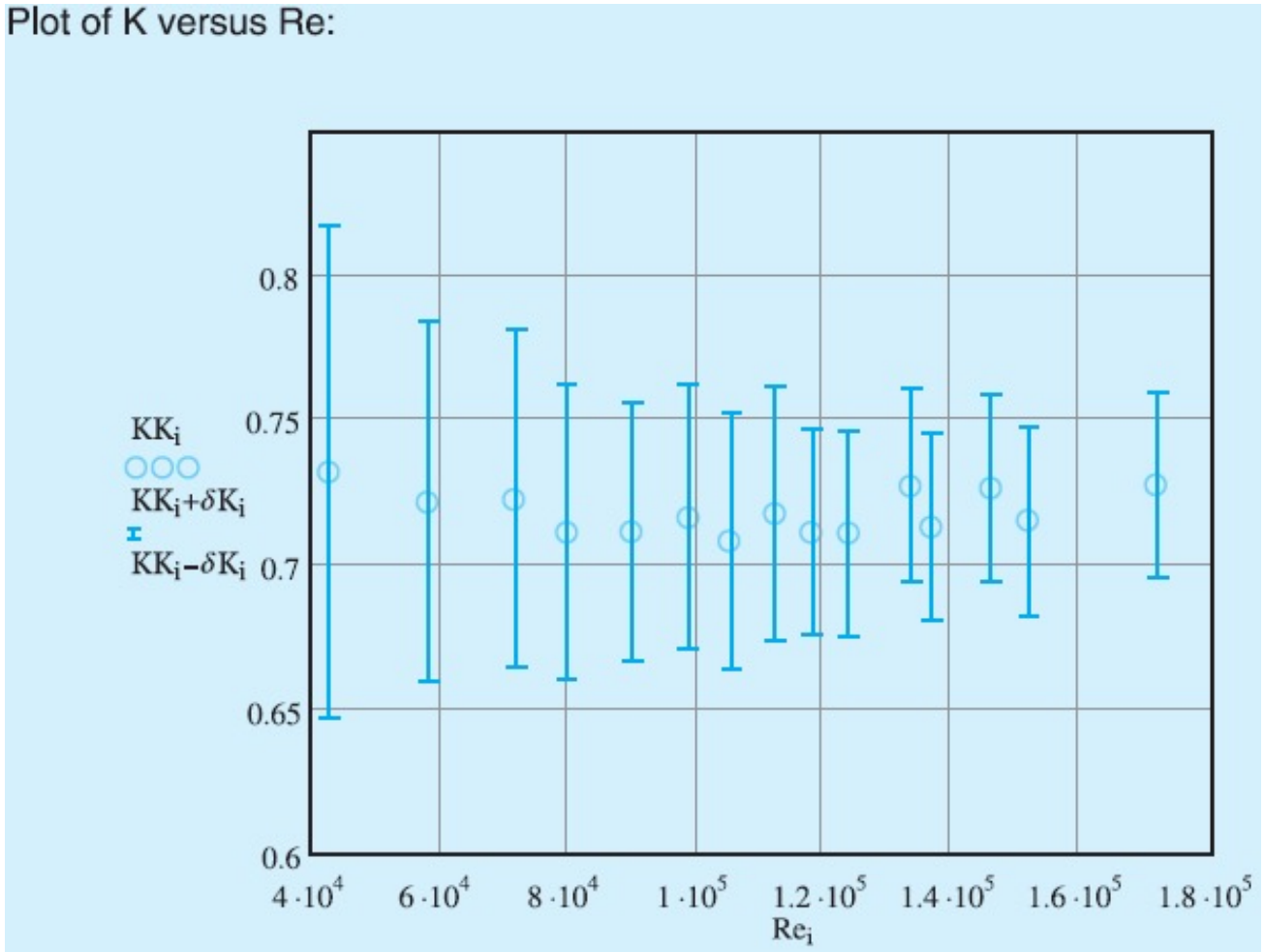

Data Acquisition and Analysis

Regression Analysis

$$Y = CX^m$$

Y is the derived result, *X* is the measurand, and *C* and *m* are constants.

$$S = \sum_{i=1}^{n} S_i^2$$

$$= \sum_{i=1}^{n} [y_i - (b + mx_i)]^2$$

$$m = \frac{\Sigma x_i y_i - (\Sigma x_i \, \Sigma y_i)/n}{\Sigma x_i^2 - (\Sigma x_i)^2/n}$$

$$b = \frac{\Sigma y_i - m \, \Sigma x_i}{n}$$

$$C = e^b$$

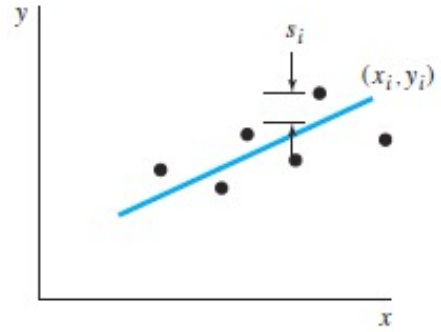

Method of least squares.

Data Acquisition and Analysis

With the data given in Example 13.1, perform a least squares regression to determine the coefficient C and exponent m in Eq. 13.5.5. Compare the result with Eq. 13.3.8.

Solution

Equations 13.5.9 to 13.5.11 are employed to evaluate C, b, and m. In Eqs. 13.5.9 and 13.5.10, x is replaced by $\ln \Delta h = \ln(h_1 - h_2)$, and y is replaced by $\ln Q$. The calculations are tabulated in the accompanying table.

i	$x_i = \ln \Delta h$	$y_i = \ln Q$	x_i^2	$x_i y_i$
1	−1.9733	−6.7338	3.8939	13.2878
2	−1.3280	−6.4253	1.7636	8.5328
3	−0.9088	−6.2146	0.8259	5.6478
4	−0.6597	−6.1058	0.4352	4.0280
5	−0.4231	−5.9875	0.1790	2.5333
6	−0.2472	−5.8925	0.06111	1.4566
7	−0.09761	−5.8293	0.009528	0.5690
8	0.007968	−5.7635	0.00006349	−0.0459
9	0.1258	−5.7138	0.01583	−0.7188
10	0.2207	−5.6665	0.04871	−1.2506
11	0.3264	−5.5913	0.1065	−1.8250
12	0.4134	−5.5675	0.1709	−2.3016
13	0.5086	−5.5017	0.2587	−2.7982
14	0.6163	−5.4632	0.3798	−3.3670
15	0.8299	−5.3391	0.6887	−4.4309
Σ	−2.5886	−87.7954	8.8374	19.3173

Substitute the summed values into Eqs. 13.5.9 to 13.5.11:

$$m = \frac{19.3173 - (-2.5886)(-87.7954)/15}{8.8374 - (-2.5886)^2/15} = 0.497$$

$$b = \frac{-87.7954 - 0.497(-2.5886)}{15} = -5.7673$$

$$C = \exp(-5.7673) = 0.00313$$

Hence the discharge is correlated to Δh by the regression curve

$$Q = 0.00313\ \Delta h^{0.497}$$

Based on the analysis performed in Example 13.1, the average value of K is 0.718. The area of the orifice is $A_0 = 9.84 \times 10^{-4}$ m². Substituting these into Eq. 13.3.8, we find that

$$Q = 0.00313\ \Delta h^{0.500}$$

Thus the two results agree quite closely. The data and regression line are plotted in Figure E13.2.

Data Acquisition and Analysis

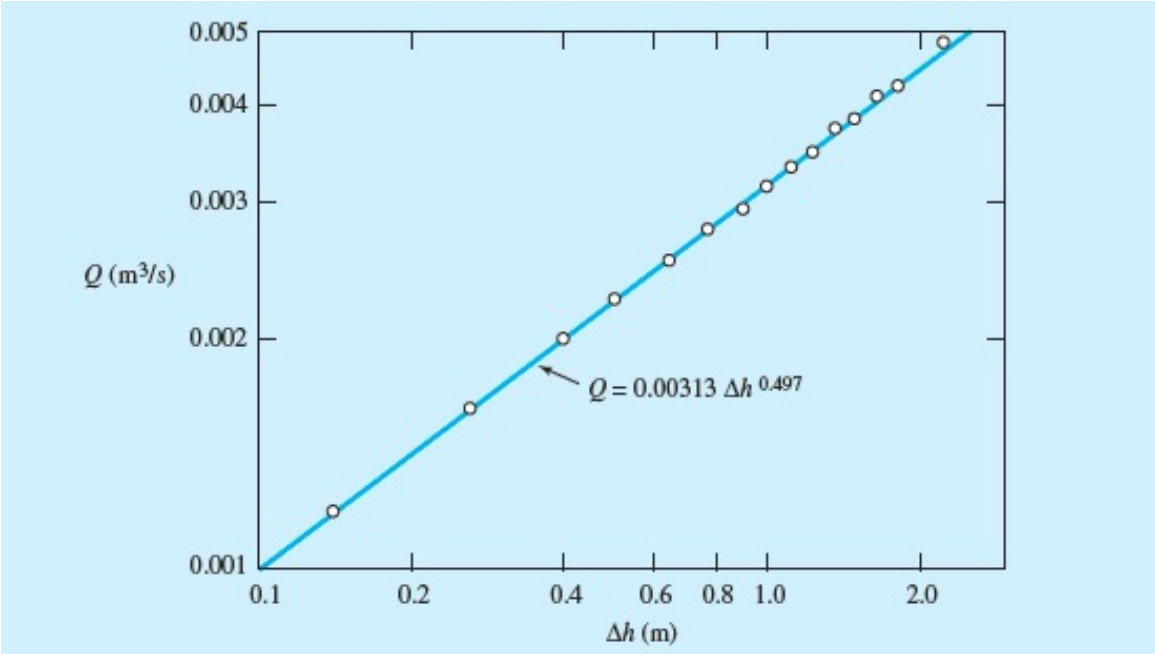

Summary

The monitoring of pressure and velocity at discrete locations in flow fields was discussed, followed by descriptions of integrated flow rate or discharge measurements.

Flow visualization is an important technique that is employed in both industrial and research laboratories to study complex flow fields, especially turbulent ones.

Today, a significant number of measurements are automated and may require analog or digital interfacing with data loggers or personal computers.